Polymer 51 (2010) 2755–2762

Contents lists available at ScienceDirect

Polymer

journal homepage: www.elsevier.com/locate/polymer

Novel ultraviolet-opaque, visible-transparent and light-emitting ZnO-QD/silicone composites with tunable luminescence colors

Yang Yang [a], Wan-Nan Li [a], Yong-Song Luo [a], Hong-Mei Xiao [a], Shao-Yun Fu [a,b,*], Yiu-Wing Mai [c,*]

[a] Technical Institute of Physics and Chemistry, Chinese Academy of Sciences, Beijing 100190, PR China
[b] International Centre for Materials Physics, Chinese Academy of Sciences, Shenyang 110016, PR China
[c] Centre for Advanced Materials Technology, School of Aerospace, Mechanical and Mechatronic Engineering J07, The University of Sydney, Sydney, NSW 2006, Australia

ARTICLE INFO

Article history:
Received 21 September 2009
Received in revised form
3 February 2010
Accepted 27 March 2010
Available online 7 April 2010

Keywords:
Composites
Luminescence
Silicone resins

ABSTRACT

Multifunctional, ultraviolet (UV)-opaque, visible-transparent and light-emitting materials with tunable luminescence colors are highly desirable for many applications in areas of ultraviolet shielding, light-emitting diodes and optical lenses etc. In this work, ZnO quantum dots (ZnO-ODs) with various sizes are first synthesized using a simple sol–gel route and novel multifunctional ZnO-QD/silicone composites with tunable luminescence colors are then prepared via a simple direct mixing method by uniformly dispersing ZnO-QDs in the silicone matrix. The structure and morphology of the ZnO-QD/silicone composites are characterized using high resolution transmission electron microscopy and attenuated total reflection Fourier transform infrared spectroscopy. UV–vis spectrometer and fluorescent photometer are used to study the optical properties of ZnO-QD/silicone composites. The results show that the ZnO-QD/silicone composites are opaque in the UV region, transparent in the visible region and also light-emitting with tunable luminescence colors from blue to yellow–green.

1. Introduction

Ultraviolet (UV) radiation causes sun-tanning and sun-burn [1–4]. Sun-tanning is caused by both UV-A (400–320 nm) and UV-B (320–290 nm) radiation while sun-burn is mainly caused by UV-B radiation [1,4]. During the past decades, the ozone layer has long been depleted and the ultraviolet radiation dosage profoundly increased owing to changes in atmospheric composition [5,6]. UV exposure can cause skin cancer, accelerate aging of skin through the formation of wrinkles and blotches, and induce other deleterious effects on the human skin [5,7]. However, UV rays are often used to excite visible lights in the development of light-emitting diode (LED) devices [8–12]. Encapsulating materials, such as epoxy resin, etc, do not filter UV rays; and UV light may leak from these materials to harm the human skins or eyes. Hence, many studies have focused on the development of UV-shielding materials, especially composites [6,13–16]. In many applications like UV-shielding windows, contact lenses and encapsulating materials, bulk transparent materials with high UV-shielding efficiency are desirable. In recent studies [6,13–16], polymer matrices used to prepare UV-shielding composites include epoxy resins, poly(styrene butylacrylate), polymethylmethacrylate, etc., which are not UV-resistant. Hence, it is necessary to develop truly transparent UV-shielding composites based on UV-resistant polymers in bulk forms suitable for UV-protection applications. In this investigation, a UV-resistant transparent silicone resin is selected to prepare multifunctional silicone composites with excellent UV-shielding capability.

ZnO is an important and attractive semiconducting material. As a light-emitter, it can ensure efficient excitonic emission at room temperature [17,18]. Nano-ZnO has many significant physical and chemical properties like high catalysis activity, high strength, chemical stability, high luminous transmittance, low dielectric constant, effective anti-bacterial and bactericide, and intensive ultraviolet absorption [15,19]. Hence, nano-ZnO can be applied to catalysts, gas sensors, semiconductors, piezo-electric devices, field-emission displays, photo-protective or UV-shielding materials, etc [20–22]. Since Spanhel and Anderson [23] investigated the growth of colloidal ZnO nanoparticles using zinc acetate anhydrate and lithium hydroxide as starting materials and ethanol as solvent, this route has been widely adopted to prepare ZnO quantum dots (QDs) in sols [8–10,24–29]. However, fine ZnO-QDs will grow continuously during storage, even stored at 0 °C, unless surface modification is applied. To avoid continuous growth of ZnO-QDs, capping agents, e.g., 3-aminopropyltrimethoxysilane, mercaptosuccinic acid and tetraethyl orthosilicate, are used to cap the ZnO-QDs to

* Corresponding authors. Technical Institute of Physics and Chemistry, Chinese Academy of Sciences, Beijing 100190, PR China. Tel./fax: +86 10 62659040.
E-mail addresses: syfu@mail.ipc.ac.cn (S.-Y. Fu), yiu-wing.mai@sydney.edu.au (Y.-W. Mai).

0032-3861/$ – see front matter © 2010 Elsevier Ltd. All rights reserved.
doi:10.1016/j.polymer.2010.03.056

slow down the particle growth in sols [30]. Polymers such as poly (vinyl pyrrolidone) [31], poly(ethylene glycol) [32,33], polystyrene [34], poly(ethylene glycol methylether) [35], poly(methylmethacrylate) [18,36–38] poly(hydroxyethyl-methacrylate) [39] and polyethylene oxide [40] are also used as capping molecules to restrict the growth of ZnO nanocrystals. But only limited work has been reported on bulk ZnO-QD/polymer nanocomposites, in which the polymer matrix will restrict the growth of the ZnO-QDs [6,8,9,18].

Silicone is a kind of transparent thermosetting materials that include silicon with carbon, hydrogen, oxygen, and sometimes other chemical elements [41–43]. Silicone polymer chemistry and structure provide different types of silicones within a broad spectrum of compositions that make silicone a viable candidate for numerous high-brightness (HB) LED packaging applications [43]. Modification of polymer chemistry can produce a silicone with a refractive index between 1.38 and 1.60. Hence, silicone resins serve as alterative materials to epoxy resins in a variety of LED devices [44–46]. Compared to transparent epoxy resins, the key attributes of silicone resins include their perfect transparency in the visible region, controlled refractive index (RI), high optical clarity, excellent thermal stability and UV-resistance [43,47]. But silicone resins do not filter UV rays which may leak out from the LED devices to harm human skins or eyes. Thus UV-shielding inorganic materials like ZnO, TiO_2 and SiO_2 [48,49] can be used to overcome this deficiency. ZnO-QDs are excellent photo-luminescent semiconductors which can emit high luminescence with colors from blue to yellow under the excitation of UV light [6,23,32,35]. Hence, the combination of quantum-sized ZnO particles as nano-filler and silicone as matrix is of scientific and technological significance since the composites may show the high luminescence of quantum dots and complementary merits of silicone resins. However, fabrication of UV-shielding and light-emitting ZnO-QD/silicone composites has not been reported till now and the preparation of bulk transparent and luminescent ZnO-QD/silicone composites remains a challenge. This is because increased thickness may readily result in opaqueness/translucence and tuning of luminescence colors is difficult since the ZnO-QDs may grow or aggregate during the preparation of composites [6,9,18].

In this study, preparation of bulk transparent ZnO-QD/silicone composites with tunable luminescence colors is reported for the first time by directly and homogeneously dispersing the as-prepared ZnO-QDs in a transparent silicone matrix. Direct dispersion of ZnO-QDs without drying in the silicone matrix effectively avoids the growth and aggregation of fine quantum dots. The choice of silicone resin as the matrix, as explained above, is due to its high optical transmittance, superior thermal stability and excellent UV-resistance. ZnO-QDs with different sizes are used to tailor the UV-shielding and luminescent properties of these nanocomposites. Hence, in this way, multifunctional silicone composites have been prepared with a high UV-shielding efficiency covering a wide range of UV-wavelength, high visible transmittance and attractive photo-luminescent properties.

2. Experimental work

2.1. Materials and sample preparation

The ZnO quantum dots (ZnO-QDs)/silicone composites were prepared via a simple direct dispersion method as illustrated in Fig. 1. Step 1 involves the synthesis of colloidal ZnO-QDs, and precipitation, purification and dispersion of the ZnO-QDs in acetone. Zn (II) solution (0.1 M) was prepared by refluxing Zn $(Ac)_2 \cdot 2H_2O$ in ethanol at 80 °C for 2 h under continuous stirring at atmospheric pressure, and then directly cooled to 0 °C. Meanwhile, a given amount of $LiOH \cdot H_2O$ was dissolved in ethanol

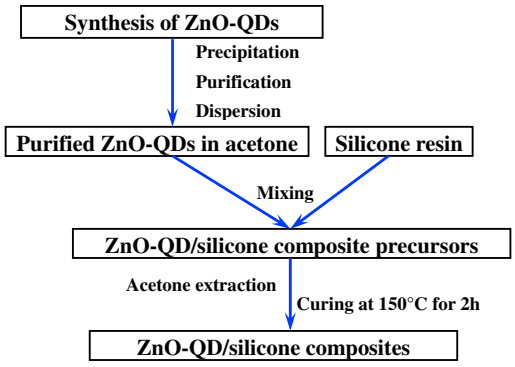

Fig. 1. Schematic diagram for preparation of ZnO-QD/silicone composites.

by ultrasonic technique and then cooled down to 0 °C. The above two solutions were mixed at a temperature of around 0 °C, followed by extensive stirring for several minutes to obtain a transparent colorless solution containing ZnO-QDs. Three different sizes (denoted by Z1, Z2 and Z3) of ZnO-QDs were synthesized, respectively, under the molar ratio of $[LiOH]/[Zn^{2+}]$ with a value of 3.5 (Z1) and 1.4 (Z2) at the mixing temperature of 0 °C while Z3 was under the molar ratio of 1.4 at 40 °C. A few drops of water were added under vigorous stirring to precipitate ZnO-QDs. The precipitated ZnO-QDs were purified by ethanol and then dispersed in 50 mL acetone. Step 2 involved mixing ZnO-QDs in acetone with silicone (Dow Corning OE 6665) via constant stirring. An extensive ultrasonic process was applied for 0.5 h until the mixture was transparent. In Step 3, the vacuity technique was used to remove solvent and the samples were prepared by pouring the resultant mixture into a steel mould followed by curing in an oven at 150 °C for 2 h. The as-prepared samples had a bulk thickness of about 4 mm.

2.2. Measurement and characterization

High resolution transmission electron microscope (HRTEM) images of ZnO-QDs and ZnO-QD/silicone composites were taken on a JEOL JEM-2010 HRTEM operated at 200 kV. Sliced thin sections of ZnO-QD/silicone composites with a thickness of about 60–80 nm, prepared by ultra-microtomy, were used to take the HRTEM images of the composites. Attenuated total reflection Fourier transform infrared (ATR-FTIR) spectra of the samples were obtained with a Varian 3100 spectrometer. Thermo-gravimetric (TG) analyses of neat silicone and the ZnO-QD/silicone composites were conducted on Netzsch STA 409 from room temperature to 1000 °C at a heating rate of 10 °C/min under an inert N_2 atmosphere. The transmittance in UV and visible regions of neat silicone and silicone composites was examined using a UV–vis spectrometer (Hitachi U-3900). The UV–vis spectrometer was also used for detecting the absorbance of ZnO-QDs. The luminescent properties of the ZnO-QDs and the ZnO-QD/silicone composites were also measured using a fluorescent photometer (Hitachi F-4600).

3. Results and discussion

Fig. 2 shows high resolution transmission electron microscopy (HRTEM) images of ZnO-QDs with different sizes and the insets show their lattice fringes and selected area electron diffraction (SAED) patterns. ZnO-QDs appear to be in the single crystal domain state and the lattice fringes show a *d*-spacing of 0.26 nm for the (002) reflection belonging to the wurtzite structure of ZnO [50]. The particle sizes were estimated by counting over 100 ZnO nanocrystals

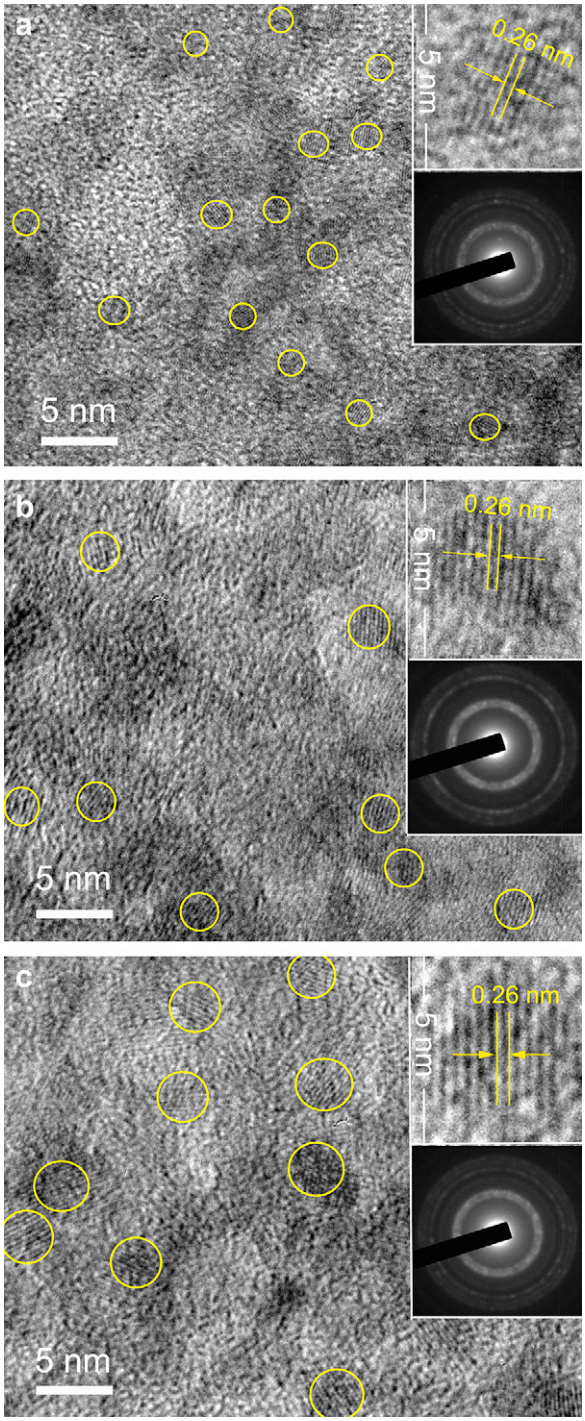

Fig. 2. HRTEM micrographs with electron diffraction image and SAED pattern in the insets of as-prepared ZnO-QDs with different sizes. (a) Z1, diameter = 1.97 ± 0.23 nm, (b) Z2, diameter = 3.03 ± 0.12 nm, and (c) Z3, diameter = 3.91 ± 0.16 nm.

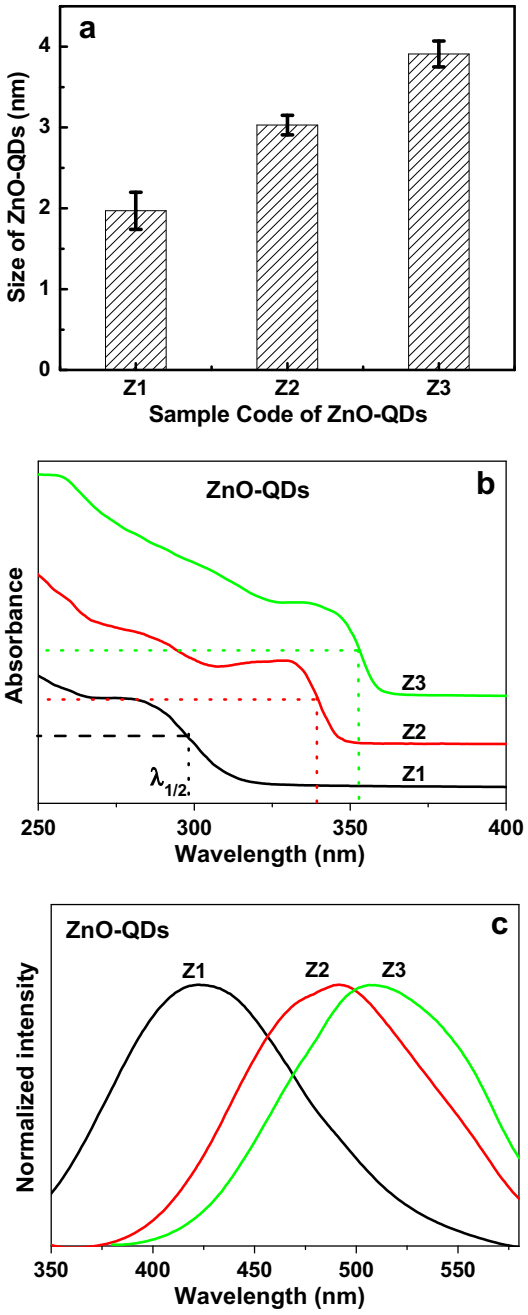

Fig. 3. (a) Size of ZnO-QDs, (b) UV–vis absorbance, and (c) PL spectra of ZnO-QDs in ethanol solution under the excitation of UV light at λ = 302 nm.

for each case from HRTEM images using the software SemAfore 4.0. The average particle diameters are: Z1 = 1.97 ± 0.23 nm, Z2 = 3.03 ± 0.12 nm, and Z3 = 3.91 ± 0.16 nm, respectively. The size versus sample code is shown in Fig. 3a.

The UV–vis absorbance spectra of the ZnO-QDs (Z1, Z2 and Z3) prepared under different synthesized conditions are shown in Fig. 3b. These spectra provide a simple way to investigate particle sizes [25]. Based on the experimental relationship between average particle diameter (D) and absorption shoulder ($\lambda_{1/2}$), defined as the wavelength at which the absorption is 50% of that at the excitonic peak, of ZnO composite colloids obtained by Meulenkamp [25] and given below:

$$1240/\lambda_{1/2} = 3.301 + 294.0/D^2 + 1.09/D \quad (1)$$

where λ in nm and D in Å, the average diameters of Z1, Z2 and Z3 can be calculated as 1.95, 3.08 and 3.99 nm, which agree well with the sizes measured directly from the HRTEM results. Equation (1) was used to fit the results for particle sizes between 2.5 and 6.5 nm by Meulenkamp [25] and here it has been extended to 1.95 nm Fig. 3c shows the visible luminescent spectra of Z1, Z2 and Z3 in ethanol with broad emission bands peaking at 425, 491 and 509 nm, indicating a red-shift as the ZnO-QDs grow in size.

Fig. 4 shows the HRTEM images of the ZnO-QDs/silicone composites having Z2 with three different loading of 0.16, 0.40 and 0.80 wt%. The direct dispersion of ZnO-QDs without drying in the silicone matrix has led to good dispersity in the polymer matrix (Fig. 4a–c). However, agglomeration cannot be completely avoided and a few aggregates are also observed (Fig. 4d–f). The phenomenon of agglomeration is common for fine ZnO-QDs (sizes of a few nanometers) dispersed in polymer matrices even if the particle surface has been properly modified to improve the dispersity [6]. This is because ZnO-QDs exhibit an enormous surface area which is several orders of magnitude larger than the surface area of conventional micro-particles. The surface area increases with the decrease of particles size and the larger surface area leads to a stronger tendency for the finer ZnO-QDs to form aggregates.

Fig. 5 shows the attenuated total reflection Fourier transform infrared (ATR-FTIR) spectra of ZnO-QDs, neat silicone resin and ZnO-QD/silicone composites. All the silicone samples show strong double peaks in the range 1130–1000 cm^{-1} as marked belonging to

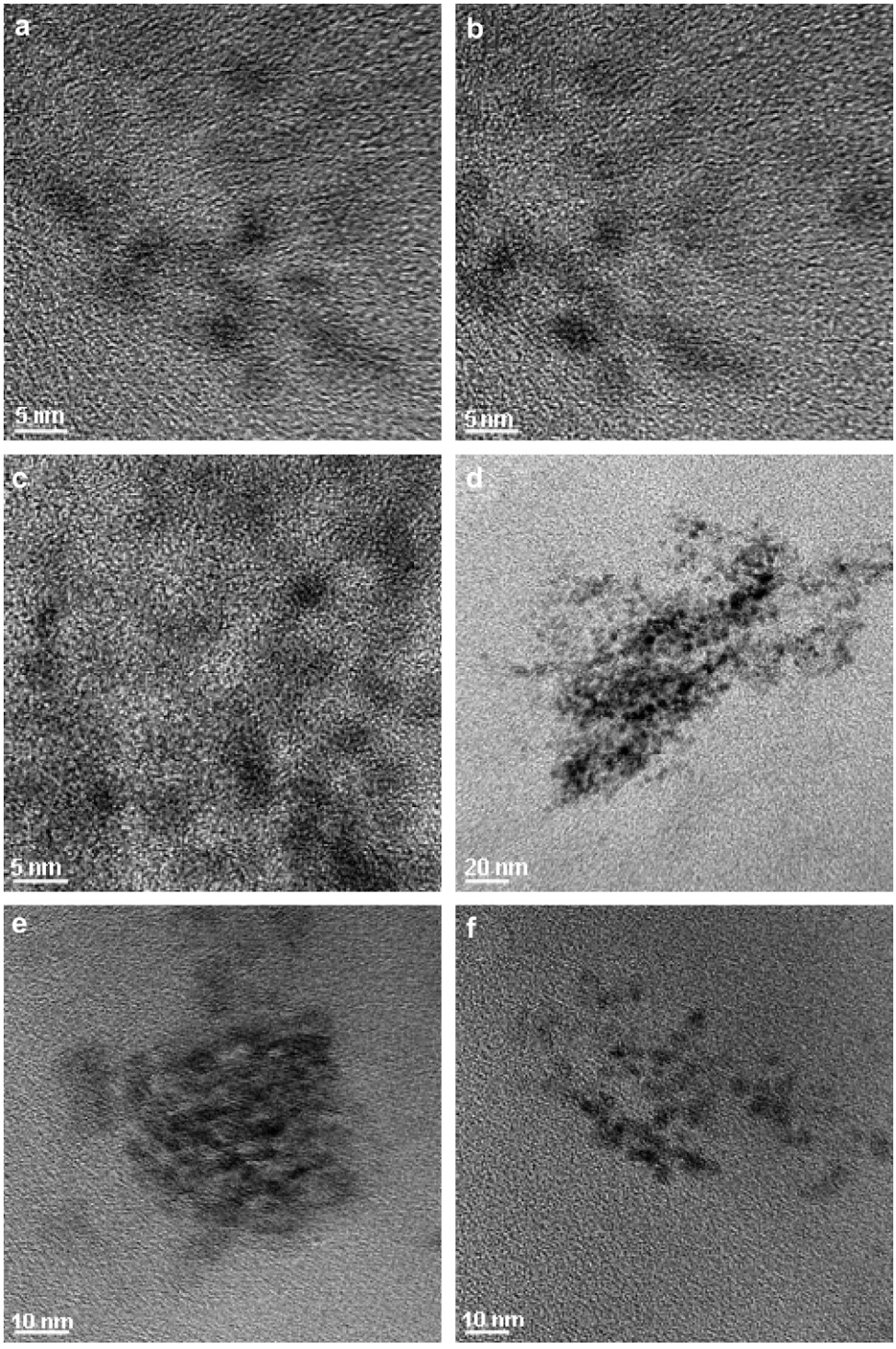

Fig. 4. HRTEM images of cross-sections of ZnO-QD/silicone composites with three different Z2-ZnO-QDs loadings: (a,d) 0.16 wt%, (b,e) 0.40 wt% and (c,f) 0.80 wt%.

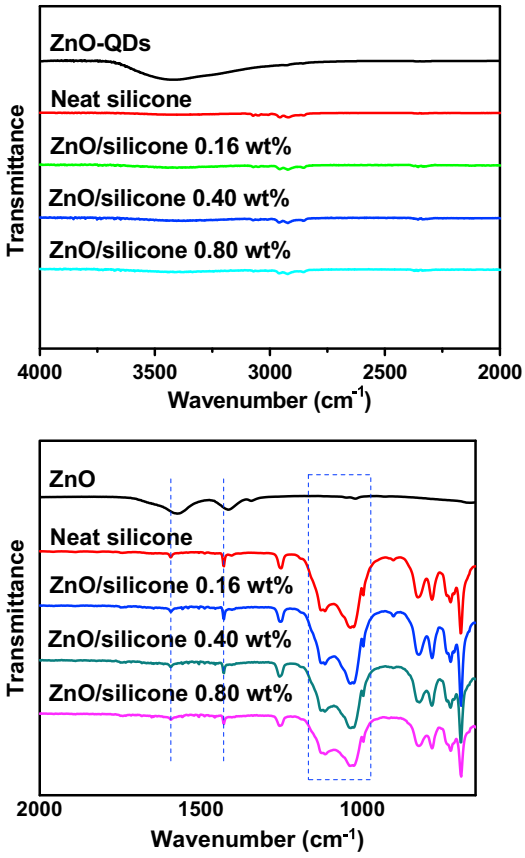

Fig. 5. ATR-FTIR spectra of ZnO-QDs, neat silicone and ZnO-QD/silicone composites.

the Si–O–Si band. The ZnO-QD/silicone composites show similar spectra with neat silicone resin, indicating that the addition of ZnO-QDs in the low loading range investigated does not obviously affect the structure of the silicone resin. In the spectra for the composites, there are no observable peaks which belonged to ZnO-QDs possibly due to its very low loading.

The UV–vis spectra of the silicone and the ZnO-QD/silicone composites are shown in Fig. 6. According to these spectra, silicone resin absorbs little UV light with a wavelength greater than about 284 nm while the silicone composites show a significant red-shift in the spectra with increasing ZnO-QDs loading and particle size. Further, the visible light transmittance decreases with increasing ZnO loading, which may suggest possible formation of aggregates in the composites [9,39,51]. This has been confirmed by the HRTEM images of the composites (Fig. 4).

The intensity of the transmitted light (I) through the composites due to light scattering can be estimated by [52]:

$$I/I_0 \propto \exp\left[\frac{-3V_p x r^3}{4\lambda^4}\left(\frac{n_p}{n_m}-1\right)\right] \quad (2)$$

which applies to spherical particles with a radius r and a refractive index n_p uniformly dispersed in a matrix with a refractive index n_m. I_0 is intensity of light that would pass the sample without scattering (i.e., the intensity of incoming light for non-absorbing materials), V_p particle volume fraction, λ light wavelength and x optical path length. The refractive indices of ZnO ($n = 2.0$) and silicone OE 6665 ($n = 1.53$ from the producer) are fixed. Increase in ZnO loading reduces the transmittance of the nanocomposites. As displayed in Fig. 6, the transmittance for all composites shows a decreasing trend with increasing ZnO-QDs loading. This can be understood in terms of Equation (2). Also, at relatively high ZnO loading, some aggregates form and decrease the transmittance. The studied composites are all quite transparent except Z3-ZnO-QDs with 0.40 and 0.80 wt% of ZnO-QDs (see Fig. 6c). The variations in transparency (right-hand side) correlate well with the observed transmittance (left-hand side) as displayed in Fig. 6.

Fig. 6 and Table 1 show that the UV-shielding efficiency is greatly enhanced by adding ZnO-QDs and it increases with increasing ZnO-QDs loading. For example, the transmittance of UV light (e.g., at 290 nm and 320 nm) is markedly reduced by adding ZnO-QDs in the silicone matrix, indicating that the UV-shielding capacity has been significantly improved. Further, the wavelength at which the UV-shielding efficiency is 94% increases with increasing particle size of ZnO-QDs (Table 1). That is, the UV-shielding wavelength range is increased by the ZnO-QDs size. However, Fig. 6 shows that Z1-ZnO-QDs and Z2-ZnO-QDs have similar high visible light transmittance but the transmittance for Z3-ZnO-QDs is significantly reduced especially at high particle loading. Thus, the 0.40 wt% case of Z2-ZnO-QDs displays not only an excellent UV-shielding property with a wide UV-wavelength range (94% UV-shielding efficiency at 362 nm) but also a high visible light transmittance with a relative value of 93.4% to the silicone matrix (i.e., 74.6%/79.9% at 600 nm) as shown in Table 1.

ZnO/poly(styrene butylacrylate) latex composites were prepared by blending poly(styrene butylacrylate) latex with a water slurry of nano- and micro-sized ZnO particles and the ultraviolet (UV) shielding property was investigated [22]. When ZnO reached a high loading of 7 wt%, UV rays were almost shielded. But the transmittance in the visible region was dramatically decreased even if the thickness of the composite films was controlled within 64–68 μm. ZnO-QDs with a size of 2.8 ± 0.4 nm were incorporated into polymethylmethacrylate (PMMA), the high UV-shielding efficiency was obtained for UV-wavelength range up to 340 nm [6]. In another study, colloidal ZnO-QDs with a uniform particle size of ~5 nm were synthesized and blended with PMMA by solution mixing to prepare PMMA/ZnO nanocomposite films [18]. The UV–vis spectra show that a small amount of colloidal ZnO-QDs (0.80 wt%) could improve the UV-shielding capability but the UV-shielding efficiency in the UV region up to ~360 nm is lower than 50%. However, in the present study, the silicone composite containing 0.40 wt% Z2-ZnO-QDs showed much higher UV-shielding efficiency of 94% at 362 nm.

Explanations for the observation of visible transmittance for the two cases of Z1 and Z2 shown, respectively, in Fig. 6a and b are given below as a function of the particle size and particle loading. Generally, for transparent composites, visible light transmittance decreases with increasing particle size and aggregation intensity of the nanoparticles. However, aggregation increases with decreasing particle size. Thus, the two competing effects by decreasing particle size and increasing particle aggregation finally bring about similar transmittance for the Z1 and Z2 cases. In contrast, the much larger particle size of Z3 has a dominating influence on the visible transmittance, thus leading to the relatively low visible transmittance.

The thermal stability of silicone and ZnO-QD/silicone composites was examined by thermo-gravimetric (TG) analysis at a constant heating rate of 10 °C/min under an inert N_2 atmosphere and the results are shown in Fig. 7. Silicone resin (Dow Corning OE 6665) has excellent thermal stability and the onset decomposition temperature is higher than ~400 °C. Until ~975 °C, the weight loss is only 25%. ZnO-QD/silicone composites show similar TG curves as the neat silicone matrix. That is, the ZnO-QD/silicone composites exhibit excellent thermal stability because of the superbly thermal stable silicone matrix. Also, ZnO-QD/silicone composites show

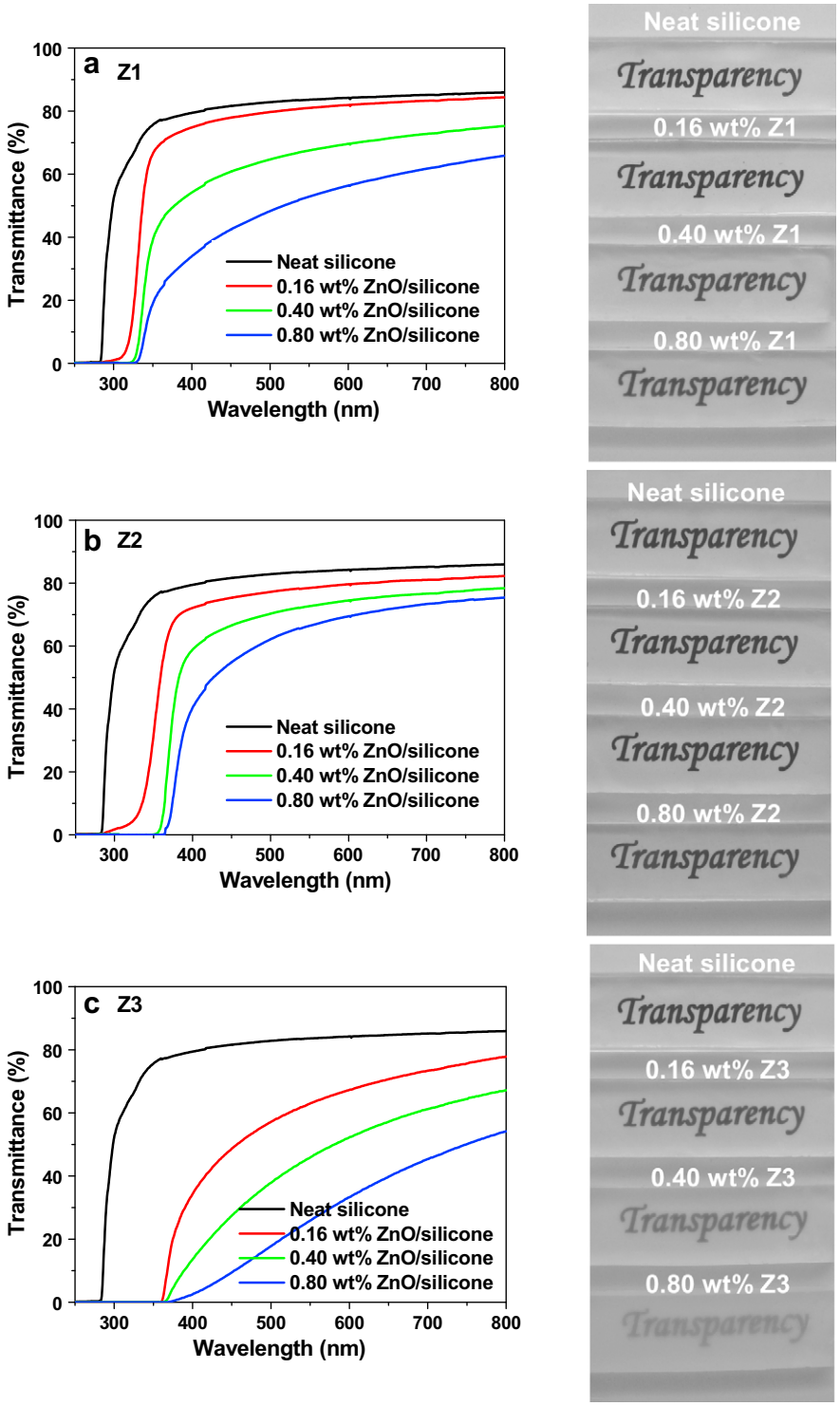

Fig. 6. UV–vis spectra and optical transparency of neat silicone and silicone composites containing ZnO-QDs of different sizes: (a) Z1, diameter = 1.97 ± 0.23 nm, (b) Z2, diameter = 3.03 ± 0.12 nm, and (c) Z3, diameter = 3.91 ± 0.16 nm.

slightly lower residual weight at high temperatures (>600 °C) than the pure silicone matrix. The observations for thermal stability are explained below.

It is well-known that silicone resin degrades to volatile low-molecular weight cyclic siloxanes in nitrogen [53]. The ZnO fillers in the polymer composites will affect the activation energy for the degradation of a polymer matrix [54]. For example, the activation energy for polyacrylate composites containing various sizes of ZnO fillers is lower than that for the polyacrylate matrix and the composite containing ZnO nanoparticles shows the lowest activation energy due to its highest catalytic effect [54]. For ZnO-QD/silicone composites, the presence of ZnO-QDs will also lower the activation energy of the silicone resin for its degradation. In contrast, ZnO particles have a higher thermal conductivity and

Table 1
Effects of particle size and loading of ZnO-QDs on transmittance.

Sample Code	Content of ZnO-QDs (wt%)	Wavelength (nm) at which UV-shielding efficiency is 94%	Transmittance at 290 nm (UV light)	Transmittance at 320 nm (UV light)	Transmittance at 600 nm (visible light)
Neat silicone	0.00	284	39.5%	65.6%	84.3%
	0.16	320	0.8%	7.5%	82.1%
Z1-ZnO/silicone	0.40	330	0.0%	0.0%	69.7%
	0.80	338	0.0%	0.0%	56.4%
	0.16	330	1.0%	3.4%	79.9%
Z2-ZnO/silicone	0.40	362	0.0%	0.0%	74.6%
	0.80	373	0.0%	0.0%	69.7%
	0.16	365	0.0%	0.0%	67.6%
Z3-ZnO/silicone	0.40	379	0.0%	0.0%	52.1%
	0.80	426	0.0%	0.0%	33.5%

a greater heat capacity value than polymers, absorbing the heat transmitted from the surrounding and thus retarding the direct thermal impact on the polymer backbones [55]. As a result, ZnO can stabilize the polymer molecules at relatively low temperatures up to ~500 °C shown in Fig. 7. Hence, pure silicone resin and composites show similar onset decomposition temperatures. However, at high temperature (e.g., 600–1000 °C shown in Fig. 7), the former activation energy effect cannot be offset by the latter thermal effect. Consequently, the existence of ZnO-QDs in silicone composites will lower the residual weight of the silicone resin.

Conversely, it was shown that the onset temperature for decomposition of PMMA was ~236 °C and the addition of 0.20 wt% to 0.80 wt% ZnO-QDs enhanced the onset temperature to between 250 and 285 °C [18]. Similar thermal stability was observed in another study on ZnO-QDs/PMMA composites [6]. Therefore, despite the increase in the onset temperature, the thermal stability of PMMA nanocomposites is much lower than that of the silicone composites reported here. In a separate investigation on epoxy composites, although the onset temperature for neat epoxy at ~360 °C was quite high, its decomposition was fast with a weight loss of ~40% at ~400 °C [56]. Hence, the ZnO-QD/silicone composites synthesized in the present work have the best thermal stability compared to other composites published elsewhere [6,18,56].

Fig. 8a shows the photo-luminescence (PL) emission spectra of the ZnO-QDs/silicone composites containing 0.40 wt% ZnO-QDs under the excitation of UV light at 302 nm. The PL emission spectra of the silicone composites with blue emission (Z1), blue–green emission (Z2) and yellow–green (Z3) (Fig. 8a) exhibit peaks, respectively, at 463 nm (Z1), 499 nm (Z2) and 523 nm (Z3) while the PL emission spectra of the ZnO-QDs with indigo emission (Z1), blue emission (Z2) and green emission (Z3) (Fig. 3) show peaks, respectively, at 423 nm, 489 nm and 510 nm. The red-shift of the PL emission peaks further demonstrates the increase in size and possible aggregation of ZnO-QDs. This is similar to that reported previously for epoxy and PMMA matrices [6,8,9]. It is proven, albeit indirectly, that the aggregation extent is most severe for the smallest size Z1 case since the red-shift is the highest with a wavelength difference of 40 nm. Conversely, the PL emission spectra are red-shifted as the ZnO-QDs particle size increases, leading to different colors of luminescence as shown in Fig. 8b. This also indicates that the luminescence colors can be properly tuned by controlling the size of ZnO-QDs in the silicone matrix. In the study of light-emitting PMMA composites containing 2.8 ± 0.4 nm ZnO-QDs, only the blue luminescence color was reported [6]. In epoxy composites containing ZnO-QDs with a size of 5 nm under an excitation of 320 nm, lights were reported to emit with a wavelength shorter than 400 nm [51]. In our recent work, epoxy composites with 3.1 ± 0.3 nm ZnO-QDs under an excitation of 370 nm exhibited a broad emission spectrum in the range 400–~640 nm peaked at ~442 nm [8]; epoxy composites containing ZnO-QDs/silica particles with 3 nm ZnO showed a broad fluorescence emission spectrum in the range 400–650 nm peaked at ~442 nm [9]. We believe this is the first time that transparent and light-emitting polymer composites with tunable luminescence colors are successfully fabricated and reported. Owing to their excellent overall performance, these ZnO-QD/silicone composites have potential for use in LED, UV-protection and optical sensors or optical filters.

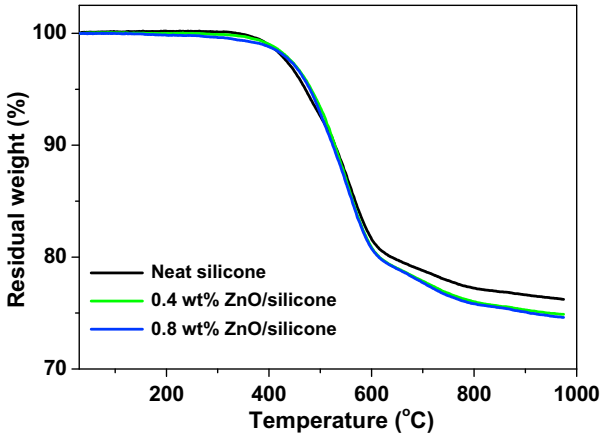

Fig. 7. Thermo-gravimetric (TG) curves of neat silicone and ZnO-QDs (Z2)/silicone composites.

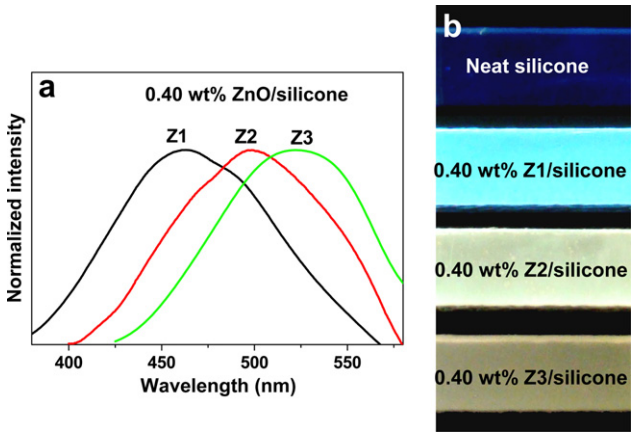

Fig. 8. (a) PL spectra and (b) digital photos of neat silicone and silicone composites containing 0.40 wt% ZnO-QDs of different sizes under the excitation of UV light at $\lambda = 302$ nm. The sample thickness is 4 mm.

4. Conclusions

Multifunctional UV-opaque, visible-transparent and light-emitting ZnO-QDs/silicone composites have been successfully synthesized in bulk form for the first time using a simple direct dispersion method. Compared to previously reported UV-shielding polymer composites, the silicone composites obtained in this work have superior thermal stability and better UV-resistance. The ZnO-QD/silicone composites at appropriate loading possess excellent UV-shielding efficiency in a wide range of UV-wavelength up to 362 nm with highly visible light transmittance. Furthermore, silicone composites with tunable luminescence colors were first time reported here. These composites have potential for applications as ultraviolet shielding and optoelectronic devices.

Acknowledgment

We thank Dr. Yuan-Qing Li and Prof. Mei-Xiang Wan for helpful discussions. This work is financially supported by the Beijing Municipal Natural Science Foundation (No. 2091004) and the National Basic Research Program of China (No. 2010CB934500).

References

[1] Epstein JH. In: Lowe NJ, Shaath NA, Pathak MA, editors. Sunscreens-development, evaluation, and regulatory aspects. 2nd ed. New York: Dekker Marcel; 1997. p. 83.
[2] Meyers DP, Lowe NJ, Scott IR. In: Lowe NJ, Shaath NA, Pathak MA, editors. Sunscreens-development, evaluation, and regulatory aspects. 2nd ed. New York: Dekker Marcel; 1997. p. 101.
[3] Kligman LH, Kligman AM. In: Lowe NJ, Shaath NA, Pathak MA, editors. Sunscreens-development, evaluation, and regulatory aspects. 2nd ed. New York: Dekker Marcel; 1997. p. 117.
[4] Masui T, Yamamoto M, Sakata T, Morib H, Adachi G. J Mater Chem 2000;10:353–7.
[5] Ries G, Heller W, Puchta H, Sandermann H, Seidlitz HK, Hohn B. Nature 2000;406:98–101.
[6] Li S, Toprak MS, Jo YS, Dobson J, Kim DK, Muhammed M. Adv Mater 2007;19:4347–52.
[7] Brash DE. Trends Genet 1997;13:410–4.
[8] Yang Y, Li YQ, Fu SY, Xiao HM. J Phys Chem C 2008;112:10553–8.
[9] Li YQ, Yang Y, Fu SY, Yi XY, Wang LC, Chen HD. J Phys Chem C 2008;112:18616–22.
[10] Li YQ, Yang Y, Sun CQ, Fu SY. J Phys Chem C 2008;112:17397–401.
[11] Narendran N, Gu Y, Freyssinier-Nova JP, Yu H, Deng L. J Cryst Growth 2004;268:449–56.
[12] Narendran N, Gu Y, Freyssinier-Nova JP, Zhu Y. Phys Status Solidi A 2005;202:60–2.
[13] Li YQ, Yang Y, Fu SY. Compos Sci Technol 2007;67:3465–71.
[14] Li YQ, Fu SY, Mai Y-W. Polymer 2006;47:2127–32.
[15] Tang E, Cheng G, Pang X, Ma X, Xing F. Colloid Polym Sci 2006;284:422–8.
[16] Xiong M, You B, Zhou S, Wu L. Polymer 2004;45:2967–76.
[17] Look DC. J Electron Mater 2006;35:1299–305.
[18] Sun D, Miyatake N, Sue HJ. Nanotechnology 2007;18:215606.
[19] Sun CQ. Prog Mater Sci 2009;54:179–307.
[20] Zhao HX, Li RKY. Polymer 2006;47:3207–17.
[21] Sawai J. J Microbiol Methods 2003;54:177–82.
[22] Xiong MN, Gu GX, You B, Wu LM. J Appl Polym Sci 2003;90:1923–31.
[23] Spanhel L, Anderson MA. J Am Chem Soc 1991;113:2826–33.
[24] Koch U, Fojtik A, Weller H, Henglein A. Chem Phys Lett 1985;122:507–10.
[25] Meulenkamp EA. J Phys Chem B 1998;102:5566–72.
[26] Sakohara S, Ishida M, Anderson MA. J Phys Chem B 1998;102:10169–75.
[27] Tokumoto MS, Briois V, Santilli CV, Pulcinelli SH. J Sol–Gel Sci Technol 2003;26:547–51.
[28] Bendre BS, Mahamuni S. J Mater Res 2004;19:737–40.
[29] Yadav HK, Sreenivas K, Gupta V, Singh SP, Katiyar RS. J Mater Res 2007;22:2404–9.
[30] Wu YL, Tok AIY, Boey FYC, Zeng XT, Zhang XH. Appl Surf Sci 2007;253:5473–9.
[31] Guo L, Yang SH, Yang CL, Yu P, Wang JN, Ge WK, et al. Appl Phys Lett 2000;76:2901–3.
[32] Abdullah M, Lenggoro IW, Okuyama K, Shi FG. J Phys Chem B 2003;107:1957–61.
[33] Abdullah M, Morimoto T, Okuyama K. Adv Funct Mater 2003;13:800–4.
[34] Chen QH, Zhang WG. J Non-Cryst Solids 2007;353:374–8.
[35] Xiong HM, Wang ZD, Liu DP, Chen JS, Wang YG, Xia YY. Adv Funct Mater 2005;15:1751–6.
[36] Khrenov V, Klapper M, Koch M, Mullen K. Macromol Chem Phys 2005;206:95–101.
[37] Sun D, Sue H. J Appl Phys Lett 2009;94:253106.
[38] Sun D, Everett WN, Wong M, Sue HJ, Miyatake N. Macromolecules 2009;42:1665–71.
[39] Hung CH, Whang WT. J Mater Chem 2005;15:267–74.
[40] Sui X, Shao C, Liu Y. Polymer 2007;48:1459–63.
[41] Narula D, Be A. Abstr Paper Am Chem Soc 1994;207:157.
[42] Ramesh K, Osman Z, Arof AK. Anti-Corro Methods and Mater 2007;54:99–102.
[43] Riegler B, Thomaier R, Bruner S. Laser Focus World 2006;42:115–8.
[44] Morita Y. J. Appl Polym Sci 2005;97:946–51.
[45] Amemiya I, Nomura Y, Mori K, Yoda M, Takasu I, Uchikoga S. J Soc Inf Display 2008;16:475–80.
[46] Ra HW, Song KS, Ok CW, Hahn YB. Korean J Chem Eng 2007;24:197–203.
[47] Huang W, Zhang Y, Yu Y, Yuan Y. J Appl Polym Sci 2007;104:3954–9.
[48] Lee RH, Huang CY, Chen CT. J Appl Polym Sci 2004;92:1432–6.
[49] Pearton SJ, Norton DP, Ip K, Heo YW, Steiner T. Prog Mater Sci 2005;50:293–340.
[50] Ge MY, Wu HP, Niu L, Liu JF, Chen SY, Shen PY, et al. J Cryst Growth 2007;305:162–6.
[51] Sun D, Sue HJ, Miyatake N. J Phys Chem C 2008;112:16002–10.
[52] Li YQ, Fu SY, Yang Y, Mai Y-W. Chem Mater 2008;20:2637–43.
[53] Jia MQ, Wu CB, Li W, Gao DH. J Appl Polym Sci 2009;114:971–7.
[54] Liufu SC, Xiao HN, Li YP. Polym Degrad Stab 2005;87:103–10.
[55] Yang TCK, Lin SSY, Chuang TH. Polym Degrad Stab 2002;78:525–32.
[56] Li YQ. PhD thesis, Graduate School of Chin Acad Sci; May 2007.